European Journal of Mechanics / B Fluids 89 (2021) 171–179

Contents lists available at ScienceDirect

European Journal of Mechanics / B Fluids

journal homepage: www.elsevier.com/locate/ejmflu

Wall friction relations in wall-bounded shear flows

E.-S. Zanoun [a,*], C. Egbers [a], H. Nagib [b], F. Durst [c], G. Bellani [d], A. Talamelli [d]

[a] LAS, BTU Cottbus-Senftenberg, D-03046 Cottbus, Germany
[b] Illinois Institute of Technology, Chicago, IL 60616, USA
[c] FMP Technology GmbH, Am Weichselgarten 34, D-91058 Erlangen, Germany
[d] CIRI Aerospace Engineering, University of Bologna, 47100 Forli, Italy

ARTICLE INFO

Article history:
Received 20 December 2020
Received in revised form 28 March 2021
Accepted 30 March 2021
Available online 8 April 2021

Keywords:
Turbulent flow
Friction law
Pipe
Channel
Flat plate boundary layer

ABSTRACT

The widespread use of available skin friction relations in engineering and in turbulence research is ample justification to examine their validities and limitations of use. The Prandtl–von Kármán logarithmic friction law (Prandtl, 1932), for instance, is vitally important for decades for predicting wall skin friction. There have been, however, rising concerns regarding its accuracy due to the deficit of the flow similarity assumption adopted in the vicinity of the wall and in the core/outer region of the flow field. Hence, the wall skin friction could possibly be doubtful when predicted using the Prandtl–von Kármán relation, in particular at high Reynolds numbers compared with values obtained from direct measurements. We therefore briefly review the recent advances in the logarithmic friction relation based on the latest pipe, channel, and boundary layer wall friction data over a wide range of Reynolds numbers. Common similarities and differences among those flows, particularly in terms of the mean flow and the wall skin friction data are highlighted. Recent pipe friction relations (Mckeon et al., 2005) are compared with the Prandtl–von Kármán logarithmic friction law and verified with new accurate pipe friction data. A revisited logarithmic skin friction relation for plane-channel flows (Zanoun et al., 2009) is reported, predicting the wall friction with an accuracy of better than ±1.44%. A modified logarithmic skin friction relation for external flows introduced by Nagib et al. (2007) is presented and discussed. We believe that having a concise review and summary of the often used friction relations in wall-bounded shear flows in a single article will be of interest to fluid mechanics readers.

Contents

1. Introduction ... 171
2. The mean velocity profile ... 172
3. The logarithmic friction law ... 173
   3.1. Pipe flow ... 173
   3.2. Plane-channel flow ... 174
   3.3. Boundary layer flow ... 176
4. Concluding remarks ... 178
   Declaration of competing interest ... 178
   Acknowledgments ... 179
   References ... 179

1. Introduction

The wall skin friction is of vital consideration in fundamental research and in practical applications. In fundamental research, the friction velocity is an important scaling parameter in wall turbulence studies. In engineering, long gas and oil pipelines motivate the examination of the skin friction relations available for flows along hydraulically smooth and rough pipe wall surfaces. Moreover, the wall skin friction accounts for approximately 50% of the total drag of a long-range subsonic airplane, and for 30% for ground vehicles [1]. Thus, accurate and preferably independent measurements of the wall skin friction with high enough spatial

* Corresponding author.
E-mail address: el-sayed.zanoun@b-tu.de (E.-S. Zanoun).

https://doi.org/10.1016/j.euromechflu.2021.03.007
0997-7546/

resolution are needed. A common method to achieve this in two-dimensional boundary layer flows is to relate the wall shear stress (τ_w) to the strain rate (dU/dy):

$$\tau_w = \mu \frac{dU}{dy}, \tag{1}$$

where y is the wall-normal distance, U is the local mean velocity, and μ is the fluid dynamic viscosity. This requires reliable velocity data within the viscous sublayer that are free from wall effects [2,3]. In most aerodynamics applications, however, the viscous sublayer is too thin to be resolved with high enough spatial resolution, making it difficult to obtain accurate velocity data within it, in particular, at high Reynolds number [4,5]. In spite of that, accurate measurements of the wall-shear stress were carried out, using the near-wall velocity data obtained by utilizing a micro-particle image velocimetry system with spatial resolution down to single-pixel ensemble correlation [4,5]. Here, one would conclude that if the size of the control volume of the measuring technique is not small enough to resolve the laminar sublayer, the so-called inertial sublayer might be used to estimate the wall skin friction [6]. Clauser [6] proposed a technique based on a claim that close to the wall, regardless of the flow geometry, a universal velocity function exists, i.e. $U = f(y, \tau_w)$ [7], and extends outside the viscous sublayer, i.e. to the inertial sublayer and behaving in a logarithmic manner; more details are given in Section 3.3.

In this paper, the logarithmic friction law is, therefore, discussed for two classes of wall-bounded shear flows, i.e ducted flow (circular pipe and rectangular channel) and flat plate boundary layer of zero pressure gradient. They are fundamentally different flows in the sense that the pipe/channel flows are fully developed whereas flat plate boundary layer are developing flows [8,9]. It is worth noting here that the logarithmic friction law in both flows has been determined based on a logarithmic scaling of the mean velocity profile at high enough Reynolds number. However, it might incorrectly predict the skin friction if inappropriate values for the logarithmic law constants, i.e. the von Kármán constant (κ) and the additive constant (B), are used [10,11]. A review of the logarithmic law constants showed variations of κ by as much as 10%, which is considered a major source of error in determining the shear stress using the logarithmic friction law if κ is not properly chosen [12]. Hence, to assess the logarithmic friction relations, new experimental data from the Cottbus large pipe, the CICLoPE pipe, and plane-channel facilities have been used.

The importance of the logarithmic law of the wall in obtaining wall friction data motivated the present authors to highlight the mean velocity profile in Section 2. A summary of some available logarithmic friction relations for fully developed turbulent pipe flow is given in sub-Section 3.1. In sub-Section 3.2, the logarithmic friction relation for plane-channel flow introduced by Zanoun et al. [13] is discussed and validated using various data sets from channel flows. New flat plate boundary layer (FPBL) wall skin friction data using the small wind tunnel facility at Brandenburg University of Technology (BTU-C-S) are presented and discussed in sub-Section 3.3. In addition, to extend the Reynolds number range for FPBL flows, the wall skin friction data from experiments at Illinois Institute of Technology (IIT) and Royal Institute of Technology (KTH) were used and are discussed. Conclusions and final remarks are given in Section 4.

2. The mean velocity profile

The law of the wall, $U^+ = f(y^+)$, was approached by Prandtl [7] using the dimensional analysis, while the velocity-defect law, $U_c^+ - U^+ = g(\eta)$, was proposed by von Kármán [14], where

Table 1
Experimental values for the logarithmic velocity profile constants (κ and B), equation Eq. (2), and the wake parameter (Π).

Flow	κ	B	Π	Reference
FPBL	0.384	4.127	0.50	[17]
Pipe	0.39	4.42	0.23	[18]
Channel	0.37	3.70	0.06	[12]

U_c^+ stands for either the normalized centerline pipe/channel local mean velocity or the freestream velocity in the case of flat plate boundary layer flow, U^+ is the normalized local mean velocity, and $\eta = y/\delta$, δ being the boundary layer thickness. On the other hand, in the inertial region, the logarithmic velocity profile was first introduced to the fluid mechanics community by von Kármán [14] from similarity arguments, while using asymptotic analysis by Milikan [15], and recently was derived by Oberlack [16] using the method of Lie-group symmetry analysis:

$$U^+ = \frac{1}{\kappa} \ln y^+ + B, \tag{2}$$

where κ is the von Kármán constant, and B is the additive constant, see Table 1.

In a more general form, Coles [19] suggested the so-called law of the wake to describe the mean velocity distribution in both the overlap and outer regions:

$$U^+ = \frac{1}{\kappa} \ln y^+ + B + \frac{\Pi}{\kappa} w(\eta), \tag{3}$$

assuming that the wake function $w(\eta)$ is universal for all two-dimensional turbulent boundary layer flows which by definition $w(0) = 1$ and $w(1) = 2$, and Π is called a profile or wake parameter. Fig. 1(a) presents the inner scaling of the mean velocity profile in two ducted flows, i.e. pipe and channel, and in a flat plate boundary layer for almost the same Reynolds number. The comparison in Fig. 1(a) was, therefore, made to examine the differences in the mean velocity profiles between the two ducted flows [9], versus the flat plate boundary layer [20] with reference to the logarithmic velocity profile. Plausible agreement between the types of flows is observed along the overlap region, however, this is not the case when the comparison is made either close to the wall or to the core/outer region. Thus Fig. 1(b) is produced, indicating that the experimental velocity data deviate from the logarithmic velocity profile for wall-normal distances $y^+ \leq 150$ and $y^+ \geq 0.15R^+$ where the velocity either overshoots or undershoots the logarithmic line. Values for constants of the logarithmic line summarized in Table 1 are used with respect to flow type to estimate the deviation of the measured velocity data from the logarithmic line and are presented in Fig. 1(b). Small differences, however, observable between the two types of flows within the viscous sublayer are obtained. On the contrary, the figure indicates discernible velocity differences between both types of flows in the core/outer region. Fig. 1(b) illustrates that the deviation from the logarithmic law in the core region of the channel flow is considerably less than those for the pipe and the flat plate boundary layer flows. To be more specific, the wake parameter, Π, which measures the departure of the mean velocity from the logarithmic velocity profile in the core region in both ducted flows and flat boundary layer flow was calculated. It is estimated to be 0.5 for the boundary layer flow case [20] presented and found to be in close agreement with the value obtained by Nagib et al. [17]. On the other hand, Π for the pipe data was found to be 0.23, which is also in alignment with values obtained by Nagib et al. [17]. In a similar manner, the wake parameter in plane-channel flow was estimated and found to be 0.06, which is much smaller than values obtained for the pipe and the boundary layer flows. Thus, one might conclude based on the

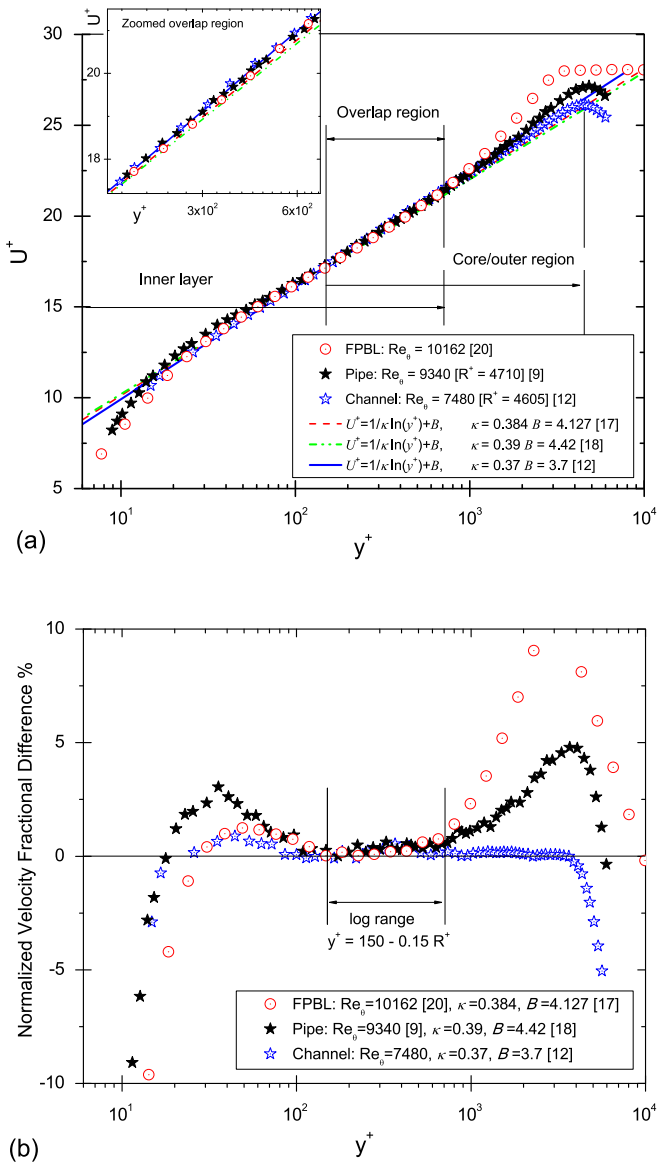

Fig. 1. (a) The inner-scaled mean velocity distribution in pipe, plane channel, and flat plate boundary layer flows compared to the logarithmic velocity profile, and (b) the normalized velocity fractional deviation from the logarithmic line in correspondence with κ and B values given in Table 1.

relative magnitude of Π in those two types of the flows that the largest deviation was observed in the flat plate boundary layer, then the pipe flow, while the channel flow showed the smallest deviation. This might be attributed to a claim made by [17] that the presence of a favorable pressure gradient in duct flows tends to make Π smaller when compared with flat plate boundary layer flows. Hence, the logarithmic law may be valid much closer to the line of symmetry of the flow in the case of the channel flow and thus can be utilized to estimate the bulk flow velocity, resulting in reliable use of Eq. (6) and/or the logarithmic friction relation, i.e. equation (10), as will be shown in Section 3.2. On the other hand, the large deviation in the core/outer region from the logarithmic velocity profile in both the pipe and boundary layer flows might result in inaccurate estimation of the wall friction using the logarithmic friction relations.

3. The logarithmic friction law

3.1. Pipe flow

The logarithmic law of the wall provides a means for estimating the wall friction. Hence it is worth briefly summarizing the recent advances in the logarithmic friction relations in wall-bounded shear flows, starting with the pipe friction law. In the pipe shear flows, the general form of the logarithmic friction law was derived by Prandtl [7] in the form:

$$\sqrt{8/\lambda} = (1/\kappa)\ln(\mathrm{Re_b}\sqrt{\lambda/32}) + B - 3/2\kappa, \tag{4}$$

based on a complete similarity assumption of the mean velocity profile in both the inner and the outer/core flow regions, where λ is called the friction factor and $\mathrm{Re_b}$ is the bulk Reynolds number defined based on the bulk flow velocity (U_b), the pipe diameter (D), and the fluid kinematic viscosity (ν). Prandtl [7] adopted a value of 0.4 for the von Kármán constant (κ), and 5.5 for the additive constant (B) based on the analysis of Nikuradse's mean velocity profiles in smooth pipe flow [21], resulting in the following known Prandtl–von Kármán logarithmic friction relation:

$$\sqrt{\frac{1}{\lambda}} = 2\log\left(\mathrm{Re_b}\sqrt{\lambda}\right) - 0.8. \tag{5}$$

Alternatively, based on a direct measure of the bulk flow velocity (U_b) and the wall shear velocity (u_τ), the following friction factor (λ) is commonly in direct use:

$$\lambda = 4C_f = 8\left(\frac{u_\tau}{U_b}\right)^2, \tag{6}$$

where C_f is the skin friction coefficient, u_τ is wall friction velocity defined as $u_\tau = \sqrt{\tau_w/\rho}$, ρ is the fluid density, and τ_w is the wall-shear stress that can be obtained either by using mean pressure gradient measurements or directly utilizing, for instance, oil film interferometry (OFI) [12,20,22]. Hence, it is worth noting here that if U_b is not precisely obtained it is a source of significant error in estimating the skin friction data.

In 1913, Blasius [23] introduced the one-seventh power law variation of the mean velocity to the fluid mechanics community, and used it to obtain the following power skin friction relation:

$$\lambda = 0.3164\ \mathrm{Re_b^{-0.25}}. \tag{7}$$

The upper limit of the Reynolds number proposed by Blasius [23] for using Eq. (7) is $\mathrm{Re_b} = 10^5$. It might be considered, however, as the lower limit for the applicability of Eq. (5) [11,24]. One might also note that the power relation is in-line with the proposed Reynolds number-dependent power law representation of the mean velocity profile by [15,25,26].

On the other hand, based on the recent pipe friction data from the Superpipe facility, McKeon et al. [10] proposed the following pipe friction relation:

$$\sqrt{\frac{1}{\lambda}} = 1.930\log\left(\mathrm{Re_b}\sqrt{\lambda}\right) - 0.537, \tag{8}$$

predicting the pipe friction for the Reynolds number range $31 \times 10^4 \le \mathrm{Re_b} \le 18 \times 10^6$.

Utilizing the new pipe facilities at BTU Cottbus-Senftenberg, and Bologna University, precise measurements of the bulk flow velocity (U_b), and the mean pressure gradient ($\mathrm{d}P/\mathrm{d}x$) along the pipe test sections were carried out in CoSmaPipe [27,28], CoLaPipe [29] and CICLoPE [30], resulting in the pipe wall friction data presented in Fig. 2, independently of the mean velocity profile measurements. Fig. 2 depicts a comparison among the

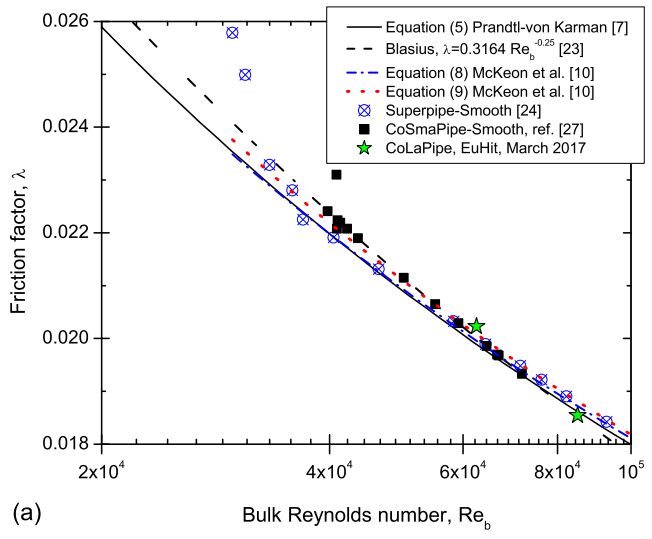

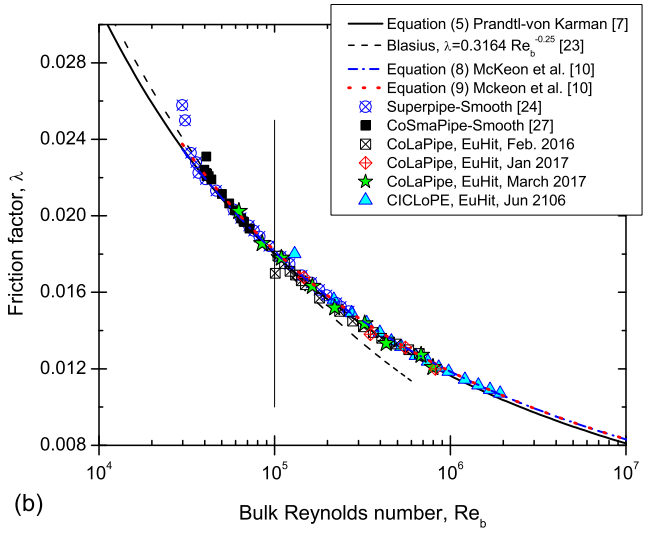

Fig. 2. The pipe friction factor, λ, versus the bulk Reynolds number, Re_b, from pipe facilities in fully developed turbulent flow regime, (a) $3 \cdot 10^4 \leq Re_b \leq 10^5$, (b) $3 \cdot 10^4 \leq Re_b \leq 2 \cdot 10^6$.

various data sets of the pipe friction versus the pipe friction relations discussed in the present paper. An overall view shows good agreement among all experimental data sets, however, further discussion is warranted. Fig. 2(a) illustrates satisfactory agreement of the present experimental data for $Re_b \leq 10^5$ with the Blasius friction relation, i.e. equation (7), within an accuracy of $\pm 1.08\%$ with reference to Eq. (7), excluding the first three data points that deviate by more than 5%. Fig. 2(b) presents data for $Re_b \geq 10^5$ compared with the various logarithmic friction relations discussed in this paper. Eq. (5) predicts the CoLaPipe wall friction data with a maximum deviation of $\pm 1.124\%$, while the maximum deviation becomes $\pm 1.56\%$ if equation (8) is considered. On the other hand, the pipe friction data from the CICLoPE facility deviate by $\pm 1.537\%$ and $\pm 0.51\%$ with respect to Eqs. (5) and (8), respectively.

Further, to correct for the deviation of the experimental data from the logarithmic friction law in the pipe flow due to the viscous effects, McKeon et al. [10] introduced the following friction relation:

$$\sqrt{\frac{1}{\lambda}} = 1.920 \log\left(Re_b\sqrt{\lambda}\right) - 0.475 - 7.04/(Re_b\sqrt{\lambda})^{0.55}. \qquad (9)$$

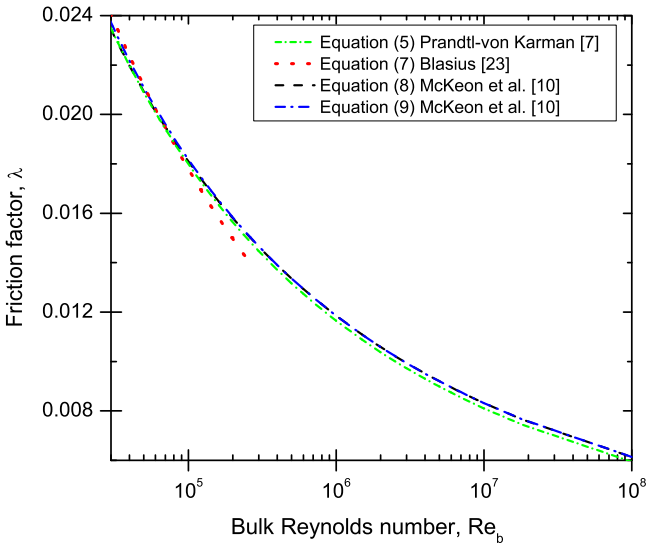

Fig. 3. Representation of the logarithmic and the power friction relations discussed in this paper.

Eq. (9) better predicts the pipe friction for the low range of the Reynolds number $Re_b \leq 10^5$ since it accounts for the wall viscous effects. It was concluded by McKeon [10] that Eq. (9) predicts the friction factor to within 1.4% of the Princeton data (0.6% at high Reynolds number, $310 \times 10^3 \leq Re_b \leq 30 \times 10^6$) and within 2.0% of the Blasius relation at low Reynolds numbers ($10 \times 10^3 \leq Re_b \leq 90 \times 10^3$). The data sets from Zanoun et al. [28] agree within $\pm 0.69\%$ when compared with Eq. (9). On the other hand, the CoLaPipe friction data for $16 \times 10^4 \leq Re_b \leq 10^6$ agree within 1.65% compared to Eq. (9), while the CICLoPE pipe wall friction data showed better agreement, i.e. within $\pm 0.5\%$, with Eq. (9) for $13 \times 10^4 \leq Re_b \leq 2 \times 10^6$ (see Table 2).

To evaluate all friction relations discussed earlier, Fig. 3 represents a comparison of the logarithmic friction relations, i.e. Eqs. (5), (8) and (9), and the power friction law, Eq. (7). From the figure, one hardly observes any differences among all the relations, however, the deviations of McKeon et al.'s [10] relations (i.e. Eqs. (8) and (9)) with respect to the Prandtl–von Kármán logarithmic law, i.e equation (5), and Blasius power relation (7) are discernible, as Fig. 4 illustrates. The difference of both logarithmic relations, i.e. Eqs. (8) and (9), introduced by McKeon et al. [10], from the Prandtl–von Kármán law increases as the Reynolds number increases. Within the present working range of the Reynolds number, i.e. $6 \times 10^4 \leq Re_b \leq 2 \times 10^6$, of both the CoLaPipe and the CICLoPE facilities, the deviation of both Eqs. (8) and (9) from the Prandtl–von Kármán law is approximately 2%, however, it increases with increasing Reynolds number, for instance, it reaches 3% at $Re_b = 2 \times 10^7$. Moreover, the friction relations of McKeon et al. [10] deviate within $\pm 2\%$ for $10^4 \leq Re_b \leq 10^5$ with respect to the Blasius power friction relationship, however, Eq. (9) behaves better for the low range of the Reynolds number.

Table 2 briefly summarises the calculated deviations in the present pipe friction measurements compared to the pipe friction relations discussed in text.

3.2. Plane-channel flow

In plane-channel flows, the two-dimensionality of the flow is expected for channels having high enough aspect ratios, i.e. width(b)-to-full height($2h$) ratio $AR = b/2h \geq 7$ [31]. In addition to flow two-dimensionality, the fully developed turbulent state in

Table 2
Summary of calculated deviations in the present pipe friction measurements compared to the pipe friction relations discussed in text.

Facility	Equation (7)[23] $Re_b \leq 10^5$	Equation (5)[7] $Re_b \geq 10^5$	Equation (8)[10] $31 \cdot 10^4 \leq Re_b \leq 18 \cdot 10^7$	Equation (9)[10] $31 \cdot 10^4 \leq Re_b \leq 6 \cdot 10^7$ $10 \cdot 10^3 \leq Re_b \leq 9 \cdot 10^4$
CoSmaPipe	±1.081%	–	±0.50%	±0.69%
CoLaPipe	±1.424%	±1.124%	±1.56%	±1.65%
CICLoPE	–	±1.537%	±0.51%	±0.5%

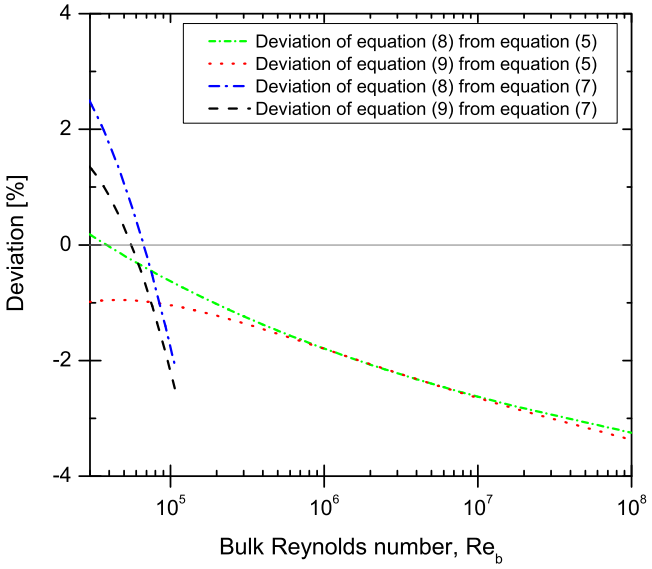

Fig. 4. Deviation of McKeon et al. [10] friction relations from the Prandtl–von Kármán [7] and the Blasius [23] friction relations.

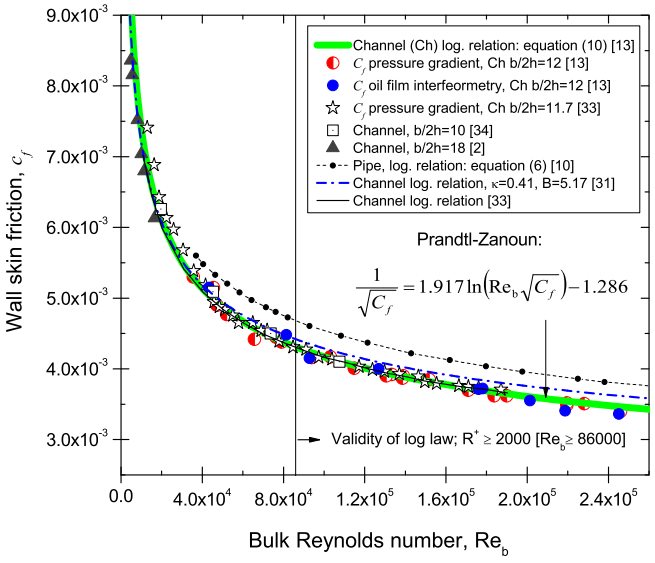

Fig. 5. Representation of the logarithmic skin friction relation, Eq. (10), compared with recent experimental results and data extracted from the literature.

channel flows is assured for long enough entrance lengths [12]. Thus, the local wall skin friction, $C_f = 2(u_\tau/U_b)^2$, data in plane-channel flow was obtained using either the mean pressure gradient or oil film interferometry where flow was assured to be fully developed. The evaluation of C_f was then established based on both measuring techniques and the results obtained are presented in Fig. 5 in the form of C_f as a function of Re_b, where Re_b is the Reynolds number defined based on the bulk flow velocity (U_b), the channel full height ($2h$), and the fluid kinematic viscosity (ν). The wall skin friction data obtained using a channel that had an aspect ratio of 12, from the mean-pressure gradient, was observed to compare well with the local skin friction measured by oil film interferometry [12]. Thus, based on those experimental skin friction data in a plane channel for $17 \times 10^3 \leq Re_b \leq 25 \times 10^4$ ($900 \leq R^+ \leq 5053$), Zanoun et al. [13] proposed the following revisited logarithmic skin friction relation:

$$\frac{1}{\sqrt{c_f}} = 1.917 \ \ln(Re_b\sqrt{c_f}) - 1.286, \qquad (10)$$

noting that it was obtained utilizing the logarithmic law of the wall by adopting a value of 0.37 for the von Kármán constant (κ), and 3.7 for the additive constant (B). It was referred to, recently, as the Prandtl–Zanoun relation by June et al. [32] taking the following modified form:

$$\frac{1}{\sqrt{\lambda}} = 2.2 \ \log_{10}(Re_D\sqrt{\lambda}) - 1.9656 \qquad (11)$$

where $\lambda = 4C_f$. They [32] defined Re_D as the Reynolds number based on the hydraulic diameter (D_h), i.e. $D_h = 4A/P$, A is the cross-sectional area of the duct, and P is the wetted perimeter.

The logarithmic friction relation, i.e. equation (10), is presented in Fig. 5 as a function of the mean-based Reynolds number, Re_b, compared with recent channel experimental results and channel data extracted from the literature. Error analysis using the least-squares method indicates that the channel experimental skin friction data deviate within ±1.44% when compared with Eq. (10). Such good agreement obtained might be attributed to the fact that the logarithmic mean velocity profile in the core region of the channel flow deviates much less than those for pipe flow, as well as for flat plate boundary layer flow as shown earlier in Fig. 1(b). This mean velocity behavior results in an accurate estimation of the bulk flow velocity, and hence, precise estimation of the wall skin friction data using either equation (6) and/or equation (10). Fig. 5 illustrates also the skin friction data obtained from mean pressure gradient measurements for $4\times10^4 \leq Re_b \leq 19\times10^4$ ($10^3 \leq R^+ \leq 4\times10^3$) in a plane channel, having an aspect ratio of 11.7:1 [33]. The following logarithmic friction relation was then proposed by Monty [33] based on his own channel experimental skin friction data:

$$\frac{1}{\sqrt{c_f}} = 4.175 \ \log_{10}(Re_b\sqrt{c_f}) - 0.416, \qquad (12)$$

which is also presented in Fig. 5. Eq. (12) agrees with Eq. (10) within an accuracy of ±0.7% for $Re_b \leq 1.2 \times 10^5$, however, its deviation increases with increasing Reynolds number, e.g. reaching 1.3% for $Re_b \approx 2.5 \times 10^5$, see Fig. 6. On the other hand, a logarithmic friction relation employing the constants proposed by Dean [31], i.e. $\kappa = 0.41$ and $B = 5.17$, exhibits less agreement with the channel experimental data and with both friction relations, i.e. Eqs. (10) and (12), in particular, for the high range of the Reynolds number. The low Reynolds number data from [34] and from [2] are also presented in Fig. 5, showing satisfactory agreement with Eq. (10). For contrast, and to emphasize the difference

between the fully developed turbulent channel and pipe flows, we have included the logarithmic friction relation, i.e. equation (8), for the pipe flow by McKeon et al. [10] which extends to very high Reynolds number, $310 \times 10^3 \leq \mathrm{Re_b} \leq 18 \times 10^6$. On the other hand, the deviation of both power friction relations proposed by Dean [31], $C_f = 0.73\ Re_b^{-0.25}$, and Zanoun et al. [13], $C_f = 0.743\ \mathrm{Re_b}^{-0.25}$, from Eq. (10) are plotted in Fig. 6. One might note that the power skin friction relation proposed by Dean [31] agrees better with Eq. (10), however, for a narrow range of the Reynolds number ($6.5 \times 10^3 \leq \mathrm{Re_b} \leq 15 \times 10^4$) when compared with the power friction relation proposed by Zanoun et al. [13].

3.3. Boundary layer flow

Along flat plate boundary layer flows, the wall skin friction (C_f) can be found by direct measurement of the wall friction velocity (u_τ), using, e.g., oil film interferometry (OFI) [22]. Alternatively, it can be obtained using Eq. (1) and/or by calculating the gradient of the momentum thickness (θ) of the boundary layer with respect to the streamwise distance (x), i.e. $\mathrm{d}\theta/\mathrm{d}x$, based on the Kármán integral momentum equation:

$$\frac{C_f}{2} = \frac{\mathrm{d}\theta}{\mathrm{d}x} = \left(\frac{u_\tau}{U_\infty}\right)^2, \tag{13}$$

where U_∞ is the free stream mean velocity. The estimation of $\mathrm{d}\theta/\mathrm{d}x$, however, requires measuring the streamwise mean velocity versus the wall-normal distances, in particular, in the vicinity of the wall at various locations along the streamwise direction of the boundary layer. It seems at first glance that it is easy to measure the local mean velocity versus the wall-normal distance, however, in most aerodynamics applications, the viscous sublayer is too thin to be resolved with high enough spatial resolution [4,5], making it difficult to obtain accurate velocity data within it, particularly, at high Reynolds number. Hence, if the control volume of the measuring technique is not small enough to spatially resolve the viscous sublayer, it is proposed that the logarithmic region of the mean velocity profile should be utilized to obtain the wall skin friction. Clauser [6], hence, introduced the following plot based on the logarithmic velocity profile:

$$\frac{U}{U_\infty} = \sqrt{\frac{C_f}{2}}\left[\Lambda\ \log_{10}\left(\frac{y u_\tau}{\nu}\right) + \Lambda\ \log_{10}\left(\frac{C_f}{2}\right)\right] + B, \tag{14}$$

where U is the local mean streamwise velocity component, $\Lambda \equiv \ln(10)/\kappa$, κ is the von Kármán constant, and B is the additive constant. It is, however, worth re-noting that the use of the Clauser plot is linked to the logarithmic velocity profile within the inertial sublayer in boundary layer flows [6]. To obtain a value for the wall skin friction utilizing the Clauser method, it is usual to superpose the Clauser plot, i.e. equation (14), on a measured velocity profile within the logarithmic range of the inertial sublayer via the adjustment of C_f as presented in Fig. 7. A proper value for the skin friction coefficient can then be obtained when the Clauser plot matches well the measured mean velocity profile within the logarithmic range, see Fig. 7. However, it is obvious from Eq. (14) that there is a direct dependence of the skin friction coefficient upon the values adopted for the von Kármán constant (κ) and the additive constant (B). Crook [35], for instance, concluded that the prediction of u_τ is sensitive to the values of κ and B adopted in the logarithmic law. He observed that a $\pm 0.5\%$ change in the slope of the logarithmic line, $1/\kappa$, results in a 12% difference in u_τ. Hence, a careful choice for the slope of the logarithmic line is an important issue in obtaining the wall skin friction using the logarithmic friction law. When the most recent and accurate values for both constants $\Lambda = 5.996$ ($\kappa = 0.384$) and $B = 4.127$ obtained [17,20] from flat plate boundary layer measurements are adopted, they would result in a rather good application of the Clauser method. It is observed, however, that the recent values for both κ and B obtained [17,20] are in very close agreement with values $\kappa = 0.3806$ ($\Lambda = 6.05$) and $B = 4.05$ obtained by careful measurements carried out by Winter and Gaudet [36]. On the other hand, the wall skin friction (C_f) results obtained utilizing equation (14) with recommended constants [17,20] were found to be in fair agreement with C_f data obtained when the most often used values $\Lambda = 5.616$ ($\kappa = 0.41$) and $B = 5.0$, proposed by Coles and Hirst [37], for flat plate turbulent boundary layers were used.

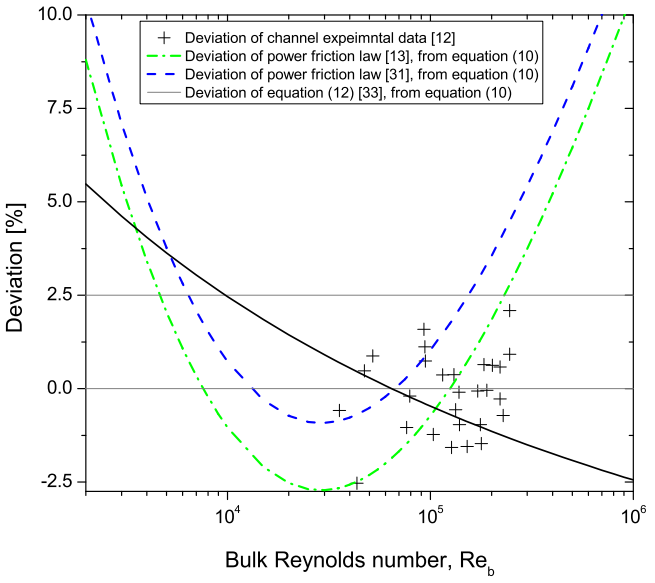

Fig. 6. Deviation of the experimental data and channel friction relations discussed in the paper from the logarithmic skin friction relation, Eq. (10), proposed by Zanoun et al. [13].

Fig. 8 presents the wall skin friction data from two measuring techniques, laser-Doppler anemometer (LDA) and oil film interferometry (OFI), versus some friction relations extracted from the literature [17,38]. The figure illustrates satisfactory agreement between the wall skin friction data obtained from the LDA near-wall mean velocity profiles and the OFI as well as with data obtained utilizing the Clauser plot. However, one might observe a little under-estimation of the wall skin friction using the OFI that might be attributed either to the accuracy of the measured oil viscosity or to the effect of the wall surface temperature at which measurements were carried out. A revisited F. Schultz-Grunow [39] logarithmic friction relation derived by Nagib et al. [17] is plotted in Fig. 8 and compared with the current experimental data. Good agreement with the modified F. Schultz-Grunow [39] relation as well as with the power friction relations [38] is obtained. One also observes from Fig. 8 the early transition to the turbulent regime at $\mathrm{Re_x} \approx 10^5$ by the artificial triggering of the boundary layer versus the natural transition at approximately $\mathrm{Re_x} \approx 5 \times 10^5$, where $\mathrm{Re_x}$ is defined based on the streamwise freestream mean velocity (U_∞), the streamwise distance (x), and the kinematic viscosity (ν).

Further examination, however, of the wall skin friction (C_f) along flat plates for high Reynolds numbers has been carried out, recently, confirming the necessity for direct and independent measurement of the wall shear stress (τ_w) [17]. Nagib et al. [17] found that many of the available empirical friction relations might describe well the local C_f behavior when modified and supported by accurate experimental data. Thus, they used the direct wall shear stress measurements of the experiments at

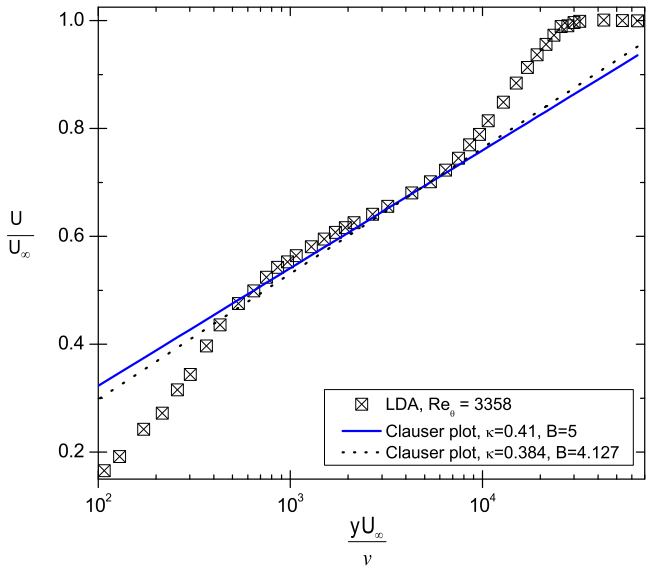

Fig. 7. The Clauser plot superposed on a selected case from the mean velocity experimental results obtained using a laser-Doppler anemometer.

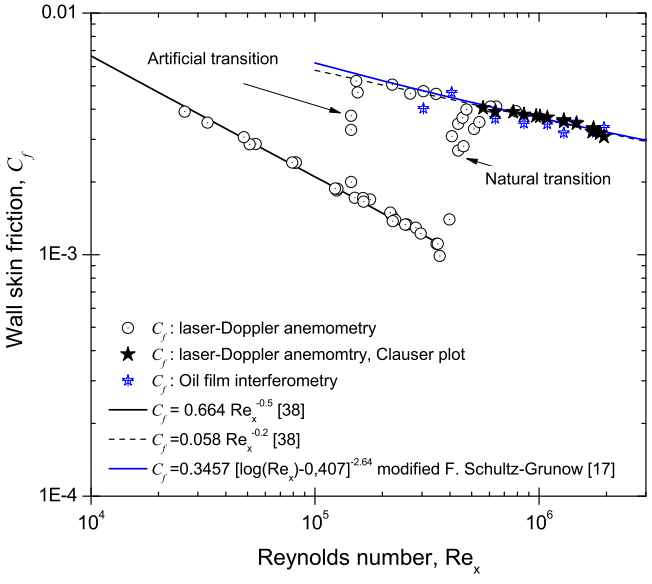

Fig. 8. Recent wall skin friction data compared with modified laminar and turbulent formulae extracted from [17,38].

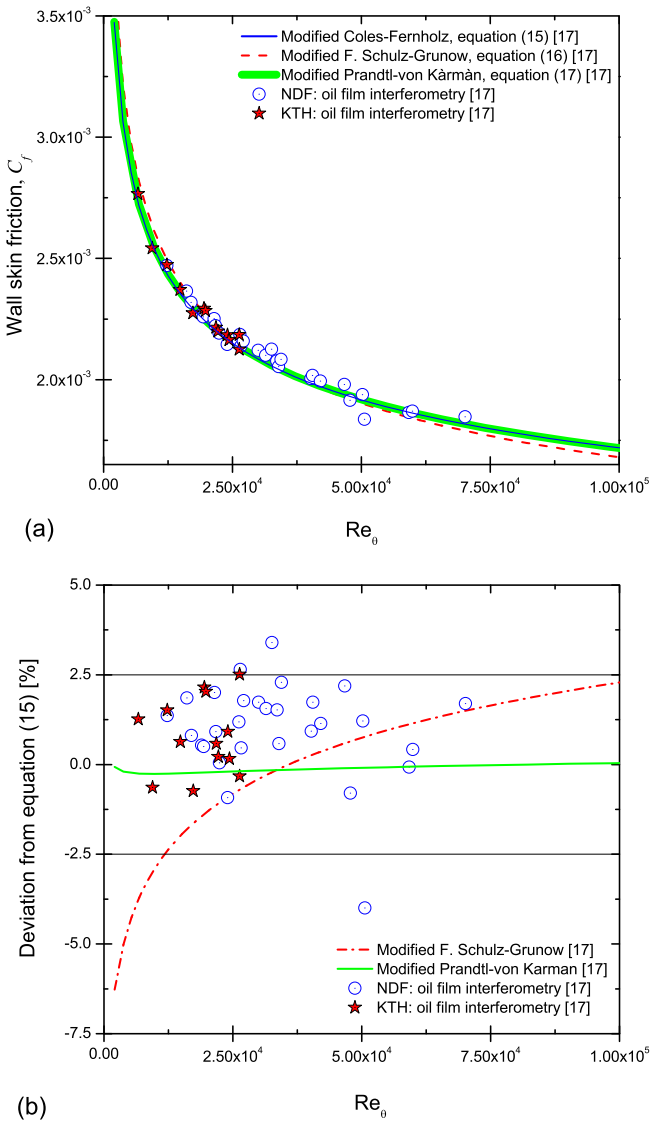

Fig. 9. The boundary layer wall skin friction, C_f, versus the Reynolds number, Re_θ:
(a) KTH and NDF experiments versus some selected friction relations [17],
(b) deviation of KTH and NDF experimental data and Eqs. (16) and (17) from Eq. (15).

Illinois Institute of Technology (IIT), Royal Institute of Technology in Stockholm (KTH) and the National Diagnostic Facility (NDF) to study the development of C_f and evaluate the quality of the various friction relations found in the literature. It was commented by Nagib et al. [17] that none of the original friction relations presented in their paper [17] were in good agreement with the recent experimental data obtained from KTH and NDF. They attributed the disagreement to the low Reynolds number effects to establish appropriate values for the coefficients required for the various forms of the skin friction relations. To revisit, for instance, a logarithmic friction relation for flat plate boundary layer flow, Nagib et al. [17] adopted Coles–Fernholz's friction relation [40]:

$$C_f = 2\,[1/\kappa\ \ln(\mathrm{Re}_\theta) + B]^{-2}\,, \tag{15}$$

for further theoretical developments. Satisfying asymptotic consideration, Nagib et al. [17] proposed new numerical values for both $\kappa = 0.384$, and $B = 4.127$ based on the collective NDF and KTH oil-film data. The modified version of Coles–Fernholz friction relation is presented in Fig. 9a and further discussed. In addition to Eq. (15), Nagib et al. [17] modified F. Schulz-Grunow [39] original friction relation to read as:

$$C_f = 0.3475\ [\log(\mathrm{Re}_x) - 0.407]^{-2.64}. \tag{16}$$

where Re_x is defined based on the freestream mean velocity (U_∞), the streamwise distance (x) measured from the leading edge, and the kinematic viscosity (ν). Moreover, Nagib et al. [17] modified the empirical coefficients of the Prandtl–Kármán skin friction relation to be written as follows:

$$C_f{}^{1/2} = 4\ [\log(\mathrm{Re}_x\sqrt{C_f})] - 2.12. \tag{17}$$

Noting that the original and modified empirical coefficients in Eqs. (15)–(17) are documented in Table 1 in Nagib et al. [17]. To be able to compare both Eqs. (16) and (17) with Eq. (15) in Fig. 9a, Re_x is related to Re_θ through the following revisited empirical

relation:

$$\mathrm{Re}_\theta = 0.012777 \cdot \mathrm{Re}_x^{0.86785} \tag{18}$$

which predicts Re_θ with an accuracy of ±1% when compared with the experimentally determined Re_θ [17]. All three selected and revisited friction relations, i.e. Eqs. (15)–(17) are plotted in Fig. 9(a), showing good agreement within the experimental accuracy. However, we find from Fig. 9(a) that the revisited version of the nearly a century old Prandtl–Kármán skin friction relation appears to be exceptionally in good agreement with Eq. (15). The good collapse of skin friction relations corrected by Nagib et al. [17] and the KTH and NDF experimental data, independent of how the flow was triggered along the flat plates and how the Reynolds number was achieved presented in Fig. 9(a), indicates a self-similarity of the wall skin friction [17].

Albeit the wall skin friction data from both NDF and KTH were directly obtained and used to evaluate the quality of the various friction relations, their deviations from Eq. (15) were estimated and presented in Fig. 9(b). The deviation of the NDF data from the revisited Coles–Fernholz friction relation, i.e. equation (15), was found to be within ±1.94%, whereas the KTH deviates within ±1.29%. Fig. 9(b) indicates also that Eq. (16) deviates within ±2.5% when compared with Eq. (15) for $1.2 \times 10^4 \leq \mathrm{Re}_\theta \leq 10^5$, however, the deviation increases for $1.2 \times 10^4 \geq \mathrm{Re}_\theta \geq 10^5$. On the other hand, the revisited version of the Prandtl–Kármán friction relation appears to be in outstanding agreement with Eq. (15) over a wide range of Re_θ.

4. Concluding remarks

Different methods to determine the wall friction in turbulent pipe, channel, and flat boundary layer flows have been reviewed. In spite of the fact that some of the methods are still under discussion the comprehensive presentation of the data may help to understand better the differences and limitations of the available logarithmic friction relations under various boundary conditions. A surprising outcome, however, of the present study is that the various data sets collected and illustrated here, fitted very well among each other and with the logarithmic friction relations presented. This, partially, might be due to the proper values chosen for constants of the logarithmic velocity profile, the high quality of the new experimental facilities and accuracy of the measuring techniques used.

In closing, from the results and discussions, we conclude that precise and independent wall skin friction data are indeed of vital importance in engineering applications, and as a scaling parameter for the analysis of wall turbulence.

The turbulent shear flows in closed conduits, i.e. circular pipe and rectangular channel, and boundary layers of zero pressure gradient are two classes of flows that are fundamentally different in the sense that pipe/channel flows are fully developed whereas boundary layers are developing flows; however, a comparison has been be made in terms of the mean velocity profiles and skin friction relations, reflecting the combined effects of flow geometry and pressure gradient. We conclude based on estimating the magnitude of the wake parameter, Π, in these two types of flows that the largest deviation in terms of the mean velocity in core region was observed in the flat plate boundary layer, then the pipe flow, while the channel showed the smallest deviation. This as claimed by Nagib et al. [17] might be attributed to the combined effects of flow geometry and favorable pressure gradient in duct flows. This observation in fact motivates further research in connection with clarifying the structural behavior of the outer layer between these two types of wall-bounded shear flows.

The Prandtl–von Kármán logarithmic friction law with $\kappa = 0.4$ and $B = 5.5$ applies for the pipe flows with reasonable accuracy. The κ value chosen is in-alignment with a recent remark made by Baumert [41] based on theoretical considerations that suggested the von Kármán constant $\kappa = 1/\sqrt{2\pi} \approx 0.399$ which is also very close to the κ–value Nikuradse [21] suggested from his measurements in 1932. In agreement with McKeon et al. [10], the results suggest that the pipe friction factor behavior falls into three regimes. For $\mathrm{Re}_b \leq 10^5$, the data are well represented by the Blasius relationship, Eq. (7). For $10^5 \leq \mathrm{Re}_b \leq 3.2 \times 10^6$, Prandtl–von Kármán's friction law, Eq. (5), applies with reasonable accuracy. For $\mathrm{Re}_b \geq 3.2 \times 10^6$, the friction relations proposed by McKeon et al. [10] yield a better description of the pipe wall friction up to the highest Reynolds number, $\mathrm{Re}_b \approx 35 \times 10^6$, achieved by Zagarola and Smits [24].

For plane channel flows, having a large enough aspect ratio, the logarithmic skin friction relation proposed by Zanoun et al. [13] with $\kappa = 0.37$ and $B = 3.7$, up to more than twice the highest Reynolds numbers available, predicts the wall skin friction with high accuracy, in particular for high Reynolds numbers. For contrast, and to emphasize the differences between the fully developed turbulent channel and pipe flows, the logarithmic friction relation, i.e. equation (8), for the pipe flow by McKeon et al. [10] which extends to very high Reynolds number was presented in Fig. 5, showing a clear difference between the two ducted flows in terms of the wall skin friction.

A revisited logarithmic skin friction relation, i.e. equation (15), with properly chosen parameters, $\kappa = 0.384$ and $B = 4.127$, by Nagib et al. [17] is accurate in representing the wall skin friction in zero pressure gradient boundary layer experiments. In addition, the revisited version of the Prandtl–von Kármán friction relation, i.e. equation (17), appears to be exceptionally in outstanding agreement when compared with Eq. (15) over a wide range of Re_θ. Finally, since the wall roughness strongly influences the above-discussed friction relations in this paper, it is of crucial importance to consider the roughness effect in an additional review.

It is worth noting here that the research work, published in this paper, required collaborations and the first author is very happy that he had the opportunity to work together with C. Egbers, H. Nagib, F. Durst, G. Bellani and A. Talamelli to get reliable measurements in pipe, channel and flat plate boundary layer flows. The pipe flow data were obtained using the CoLaPipe at BTU C-S by E.-S. Zanoun and C. Egbers, and CICLoPE at University of Bologna by G. Bellani and A. Talamelli. G. Bellani and A. Talamelli designed and prepared the CICLoPE set-up and E.S. Zanoun had an opportunity to work with both during one of the EuHit (European High-performance Infrastructures in Turbulence) campaigns in CICLoPE. The channel flow data were obtained using plane-channel facility at LSTM-Erlangen, Friedrich-Alexander-University, during the research stay of the first author working under the supervision of both F. Durst and H. Nagib. H. Nagib provided the flat plate boundary layer via his close collaboration with both KTH (Royal Institute of Technology in Stockholm) and NDF (National Diagnostic Facility). All authors contributed in writing, interpreting and discussing the data in the different sections of the manuscript.

Declaration of competing interest

The authors declare that they have no known competing financial interests or personal relationships that could have appeared to influence the work reported in this paper.

Acknowledgments

This project is funded within the DFG-Priority Programme SPP 1881 "Turbulent Superstructures", grant no. EG100/24-2. Thanks are due to Dr. Österlund for making his data available to us and also Illinois Institute of Technology (IIT) and Royal Institute of Technology in Stockholm (KTH) and the National Diagnostic Facility (NDF). Dr. Sebastian Merbold (BTU-Cottbus-Senftenberg) is thanked for comments on the manuscript.

References

[1] V.I. Kornilov, Reduction of turbulent friction by active and passive methods (review), Thermophysics and Aeromechanics 12 (2) (2005) 175–196.
[2] F. Durst, H. Kikura, I. Lekakis, J. Jovanovic, Q.-Y. Ye, Wall shear stress determination from near-wall mean velocity data in turbulent pipe and channel flows, Exp. Fluids 20 (1996) 417–428.
[3] F. Durst, E.-S. Zanoun, M. Pashtrapanska, In situ calibration of hot wires close to highly heat-conducting walls, Exp. Fluids 31 (2001) 103–110.
[4] C. Kähler, U. Scholz, J. Ortmanns, Wall-shear-stress and near-wall turbulence measurements up to single pixel resolution by means of long-distance micro-PIV, 2006, http://dx.doi.org/10.1007/s00348-006-0167-0.
[5] C. Cierpka, S. Scharnowski, C.J. Kähler, Parallax correction for precise near-wall flow investigations using particle imaging, 2013, http://dx.doi.org/10.1364/AO.52.002923.
[6] F.H. Clauser, Turbulent boundary layers in adverse pressure gradients, J. Aerosp. Sci. 2 (1954) 91–108.
[7] L.Z.L. Prandtl, Reibungswiederstand, hydrodynamische Probleme des Schiffsantriebs, herausgeg, v. G. Kempf u. E. Förster, 1932, p. 87. Neuere Ergebnisse der Turbulenzforschung, Vol. 77, Z. VDI Bd., 1933, p. 105, Nr. 5; Ergeb. Aerodyn. Versuchsanstalt Göttingen (1927) 1, 3 Lief., (English Transl. NACA TM 720).
[8] K.R. Sreenivasan, The turbulent boundary layer, in: M. Gad el Hak (Ed.), Frontiers in Exp. Fluid Mech, in: Lecture Notes in Engineering, vol. 46, Springer, Berlin, 1989, pp. 159–209.
[9] E.-S. Zanoun, F. Durst, Momentum transport and turbulent kinetic energy production in plane-channel flow, J. Mass Heat Transf. 52 (15–16) (2009).
[10] B.J. McKeon, M.V. Zagarola, A.J. Smits, A new friction factor relationship for fully developed pipe flow, J. Fluid Mech. 538 (2005) 429–443.
[11] E.-S. Zanoun, F. Durst, O. Bayoumi, A. Al-Salaymeh, Wall skin friction and mean velocity profiles of fully developed turbulent pipe flows, Exp. Therm. Fluid Sci. 32 (1) (2007) 249–261, http://dx.doi.org/10.1016/j.expthermflusci.2007.04.002.
[12] E.-S. Zanoun, F. Durst, H. Nagib, Evaluating the law of the wall in two-dimensional fully developed turbulent channel flows, Phys. Fluids 15 (2003) 3079.
[13] E.-S. Zanoun, F. Durst, H. Nagib, Refined C_f relation for turbulent channels and consequences for high Re experiments, J. Fluid Dyn. Res. 41 (2009) 1–12.
[14] Th. von Kármán, Mechanische aehnlichkeit und turbulenz, Nachr. Geswiss Goett. (1930) 68.
[15] C.M. Millikan, A critical discussion of turbulent flows in channels and circular tubes, in: Proc. 5th Int. Congress of Appl. Mech., 1938, pp. 386–392.
[16] M. Oberlack, A unified approach for symmetries in plane parallel turbulent shear flows, J. Fluid Mech. 427 (2001) 299.
[17] H.M. Nagib, K.A. Chauhan, P.A. Monkwetiz, Approach to an asymptotic state for zero pressure gradient turbulent boundary layers, Phil. Trans. R. Soc. A 365 (2007) 755–770.
[18] A.E. Perry, S. Hafez, M.S. Chong, A possible reinterpretation of the Princeton superpipe data, J. Fluid Mech. 439 (2001) 395–401.
[19] D.E. Coles, The law of the wake in the turbulent boundary layer, J. Fluid Mech. 1 (1956) 191–226.
[20] J.M. Österlund, A.V. Johansson, H.M. Nagib, M.H. Hites, Wall shear stress measurements in high Reynolds number boundary layers from two facilities, AIAA Paper, in: 30th Fluid Dynamics Conference, Norfolk, VA, 1999, pp. 99–3814.
[21] J. Nikuradse, Gesetzmössigkeiten der turbulenten Strömung in glatten Rohren, Forschg. Arb. Ing.-Wes. 356 (1932).
[22] L.H. Tanner, L.G. Blows, A study of the motion of oil films on surface in air flow, with application to the measurements of skin friction, J. Phys. E: Sci. Instrm. 9 (1976) 194–202.
[23] H. Blasius, Das Ähnlichkeitsgesetz bei Reibungsvorgängen in Flussigkeiten, Forsch. Arb. Ing. 134 (1913).
[24] M.V. Zagarola, A.J. Smits, Mean-flow scaling of turbulent pipe flow, J. Fluid Mech. 373 (1998) 33–79.
[25] M. Wosnik, L. Castillo, W. George, A theory for turbulent pipe and channel flows, J. Fluid Mech. 421 (2000) 115.
[26] N. Afzal, Power and log laws velocity profiles in fully developed turbulent pipe flows: Equivalent relations at large Reynolds numbers, Acta Mech. 151 (2001) 171–183.
[27] E.-S. Zanoun, C. Egbers, Flow transition and development in pipe facilities, J. Eng. Appl. Sci. 63 (2) (2016) 141–159.
[28] E.-S. Zanoun, M. Kito, C. Egbers, A study on flow transition and development in circular and rectangular ducts, J. Fluids Eng. 131 (2009) 1–11.
[29] F. König, E.-S. Zanoun, E. Öngüner, C. Egbers, The CoLaPipe–the new Cottbus large pipe test facility at Brandenburg University of Technology Cottbus–Senftenberg, J. Rev. Sci. Instrum. 85 (2014) 075115.
[30] T. Fiorini, Turbulent Pipe Flow High Resolution Measurements in CICLoPE (Ph.D. thesis), Universita' DI Bologna, 2017.
[31] R.B. Dean, Reynolds number dependence of skin friction and other bulk flow variables in two-dimensional rectangular duct flow, ASME J. Fluid Eng. 100 (1978) 215.
[32] J. June, B. Bertolucci, L.N. Cattafesta, M. Sheplak, Diagnostic Techniques to Elucidate the Aerodynamic Performance of Acoustic Liners, NASA/CR–2017–219583, 2017, pp. 1–124.
[33] J.P. Monty, Developments in Smooth Wall Turbulent Duct Flows (Ph.D. thesis), The University of Melbourne, Australia, 2005.
[34] K.T. Christensen, Experimental Investigation of Acceleration and Velocity Fields in Turbulent Channel Flow (Ph.D. thesis), Department of Theoretical and Applied Mechanics, University of Illinois at Urbana-Champaign, IL, USA, 2001.
[35] A. Crook, Skin-Friction Estimation at High Reynolds Numbers and Reynolds-Number Effects for Transport Aircraft, Center for Turbulence Research Annual Research Briefs, 2002.
[36] K.G. Winter, L. Gaudet, Turbulent boundary-layer studies at high Reynolds numbers at Mach numbers between 0.2 and 2.8, ARC R & M 3712, 1970.
[37] D.E. Coles, E.A. Hirst, Computation of turbulent boundary Layers-1968, in: D.E. Coles, E.A. Hirst (Eds.), Proceedings of AFOSR–IFP–Stanford Conference, Vol. 2, Thermosciences Div. Dept. of Mechanical Engineering, Stanford Univ. Stanford, CA, 1969.
[38] H. Schlichting, Boundary Layer Theory, seventh ed., McGraw-Hill, New York, NY, 1979.
[39] F. Schultz-Grunow, New Frictional Resistance Law for Smooth Plates, NACA TM 986, 1940.
[40] H.H. Fernholz, P.J. Finley, The incompressible zero-pressure gradient turbulent boundary layer: an assessment of the data, Prog. Aerosp. Sci. 32 (1996) 245–311, http://dx.doi.org/10.1016/0376-0421(95)00007-0.
[41] H.Z. Baumert, Universal equations and constants of turbulent motion, Phys. Scripta 2013 (2013) The Royal Swedish Academy of Sciences, T155.